S_1 and S_2 Excited States of Gas-Phase Schiff-Base Retinal Chromophores: A Time-Dependent Density Functional Theoretical Investigation

Mengtao Sun,*,† Yong Ding,‡ Ganglong Cui,§ and Yajun Liu*,§

National Laboratory for Condensed State Matter Physics, Institute of Physics, Chinese Academy of Sciences, P. O. Box 603-146, Beijing 100080, China, College of Chemistry, Beijing Normal University, Beijing 100875, China, and Department of Physics, Peking University, Beijing 100871, China

Received: February 4, 2007

In concert with the recent photoabsorption experiments of gas-phase Schiff-base retinal chromophores (Nielsen et al. *Phys. Rev. Lett.* **2006**, *96*, 018304), quantum chemical calculations using time-dependent density functional theory coupled with different functionals and under the Tamm−Dancoff approximation were made on the first two excited states (S_1 and S_2) of two retinal chromophores: 11-*cis* and all-*trans* protonated Schiff bases. The calculated vertical excitation energies (T_v) and oscillator strengths (f) are consistent with the experimental absorption bands. The experimentally observed phenomenon that the transition dipole moment (μ) of S_2 is much smaller that of S_1 was interpreted by 3D representation of transition densities. The different optical behaviors (linear and nonlinear optical responds) of the excited states were investigated by considering different strengths of external electric fields.

1. Introduction

Retinal proteins (rhodopsins) are located in cell membrane and eye retina, which naturally exist in protonated Schiff-base form and can convert electromagnetic energy into chemical energy.[1] The absorption of visible light that strikes eyes can arouse in the molecule an ultrafast response. As a central issue in photobiology, understanding the intrinsic ultrafast response mechanism is a challenging work.[2,3] Because most experiments[4−6] were performed in liquid phases till the recent papers,[2,3] it is hard to decide if the ultrafast response is an intrinsic property of this class molecules or a consequence of an interaction between the molecule and environment.[7,8] Theoretically, Anfinrud[9] and co-workers have suggested a three-state (S_0, S_1, and S_2) model to explain the ultrafast photophysics process in bacteriorhodopsin. Olivucci[10] and co-workers proposed another two-state (S_0 and S_1) model and studied the related isomerization pathways on the S_1 and S_2 states in solution phase[11] and concluded that S_1 and S_2 are nearly degenerate states, which is similar to the conclusion drawn by Yamamoto[12] et al. Moreover, the S_1-S_2 level spacing is sensitive to the external perturbations and the measurements in different conditions,[4−6,13−15] and the addition of solutions makes the situation more complicated. Therefore, the S_1 and S_2 excited states' behavior in the vacuum and unperturbed conditions is very important for extracting the ultrafast response mechanism hidden in the veil.

As a specific example of retinal protein, the photoisomerization from 11-*cis* protonated Schiff base (PSB11) to its all-*trans* protonated Schiff base (PSBT) isomer (see Figure 1 for their structures) is one of the fastest chemical reactions observed so far.[7,16] Some experimental[4−6] and theoretical[11,17] studies have been reported in different solutions for understanding such a phenomenon. As a result of low target densities, few experiments were done in the gas phase. However, information related to this photoisomerization process without external perturbations is crucial for elucidating the mechanism, since it can provide us a simpler picture about the photophysical and photochemical processes than ones in solution phase.[2,3] Recently, S_1 and S_2 excited state properties of gas-phase Schiff-base retinal chromophores have been studied from the experimental viewpoints[2,3] and have also been investigated with the means of computational modeling.[18−20]

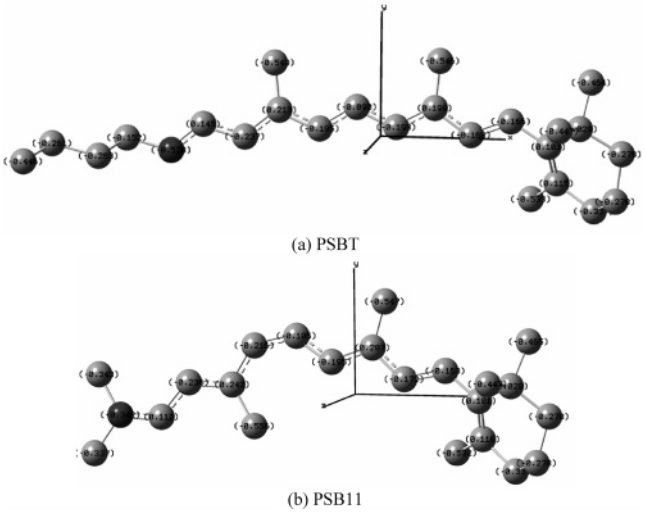

Figure 1. The schematic structure of (a) PSBT and (b) PSB11 retinal chromophores without H atoms together with the coordinate systems and B3LYP/6-31G(d) calculated Mulliken charges. For the detailed optimized geometric parameters, see Supporting Information.

In this work, the T_v, f, and μ values of the PSB11 and PSBT S_1 and S_2 excited states were calculated by time-dependent density functional theory (TD-DFT) methods in vacuum and compared with the experimental detected values.[2] The experimentally observed phenomenon that the S_2 μ value is much smaller than the S_1 one was interpreted by a 3D representation

* To whom correspondence should be addressed. E-mail: mtsun@aphy.iphy.ac.cn.
† Chinese Academy of Sciences.
‡ Peking University.
§ Beijing Normal University.

10.1021/jp0709757 CCC: $37.00
Published on Web 03/20/2007

of transition densities. The different optical behaviors (linear and nonlinear optical responds) of the excited states were investigated by considering different strengths of external electric fields.

2. Computational Details

The PSB11 ground-state geometry was fully optimized by means of the DFT[21,22] Becke's three-parameter hybrid function[23] with the nonlocal correlation of Lee−Yang−Parr[24] (B3LYP) with 6-31G(d), 6-31+G(d), and 6-311++G (d) basis sets,[25−28] respectively. The frequency analyses were done at the B3LYP/6-31G(d) and B3LYP/6-31+G(d) computational levels. The geometrical optimization and frequency analysis of the PSBT ground state was done by B3LYP/6-31G(d) and B3LYP/6-31+G(d). At the B3LYP/6-31G(d) optimized ground states' geometries, the T_v, f, and μ values of the PSB11 and PSBT S_1 and S_2 excited states were calculated by TD-DFT[29] with different functionals as the B3LYP, Becke88−Perdew−Wang91 exchange correlation functional (BPW91),[23,30] Slater−Dirac−Vosko−Wilk−Nusair exchange correlation functional (SVWN),[31,32] along with 6-31G(d), 6-31+G(d), and 6-311++G(d) basis sets. All the above calculations were performed on Gaussian03 program package.[33] The TD-DFT with the Tamm−Dancoff approximation[34] (TDA) were used with the B3LYP functional and the 6-31G(d) and 6-311G(d) basis sets to calculate the T_v, f, and μ values of the PSB11 and PSBT S_1 and S_2 excited states at their B3LYP/6-31G(d) optimized ground-state geometries. The TD-DFT/TDA jobs were completed by NWChem 4.7[35] computational chemistry package.

The 3D cube representation of transition density was used to show the orientation of the transition dipole moment.[36−39] For deciding influence effects of external static electric field F, the changes in dipole moment and polarizability upon excitations induced by irradiation are also studied by the equation of the static electric field F dependent transition energy[40,41]

$$E_{exc}(F) = E_{exc}(0) - \Delta\mu F - \frac{1}{2}\Delta\alpha F^2 \quad (1)$$

where $E_{exc}(0)$ is the excitation energy at zero field, $\Delta\mu$ is the change in dipole moment, and $\Delta\alpha$ is the change in polarizability. Meanwhile, the photoinduced dynamics of PSB11 and PSBT are further investigated with transition density, which better shows the orientation of the transition dipole moment corresponding to different transitions.

3. Results and Discussion

3.1. Ground-State Geometries. The PSB11 ground state geometry was optimized by the B3LYP method with 6-31G(d), 6-31+G(d), and 6-311++G(d) basis sets. The optimizations results indicated that the size of the basis sets hardly affect the geometric parameters. Then PSBT ground-state geometry was just optimized by B3LYP/6-31G(d) and B3LYP/ 6-31+G(d), which also showed that the basis set size hardly influences the optimization results. Hereafter, the property calculations of PSB11 and PSBT were performed under their B3LYP/6-31G(d) optimized ground-state geometries. For the detailed optimized results, please see Figure 1 and Supporting Information. The subsequent B3LYP/6-31G(d) and B3LYP/6-31+G(d) frequency analyses indicated that the optimized geometries are the total minima on the potential energy surface of PSB11 and PSBT, respectively.

3.2. S_1 and S_2 Vertical Excitation Energies and Oscillator Strengths. The T_v and f values of the PSBT and PSB11 S_1 and S_2 states were calculated by TD-B3LYP, TD-BPW91, and TD-SVWN along with 6-31G(d), 6-31+G(d), and 6-311++G(d) basis sets, respectively. The calculated results were compared with the experimental detected values in Table 1. As shown in Table 1, for both PSBT and PSB11, the basis set size has very little affect on the calculated T_v and f values. However, the different functionals of the TD-DFT method do affect the calculated T_v and f values. For the PSBT S_1 and S_2 states, the TD-B3LYP, TD-BPW91, and TD-SVWN with 6-31G(d) basis set calculated $T_v(f)$ values to be 536.1(1.561) and 393.7(0.669), 590.5(0.835) and 451.9(0.891), and 592.3(1.003) and 451.1-(1.058) nm, respectively. The corresponding calculated results for the PSB11 are 539.5(1.288) and 396.8(0.577), 590.5(0.835) and 451.9(0.891), and 596.1(0.8186) and 454.7(0.8895) nm, respectively. The experimental detected S_1 and S_2 T_v values for PSBT and the PSB11 are 620 and 385 and 610 and 390 nm[2], respectively. All TD-DFT calculated PSBT S_1 and S_2 T_v values are more or less in agreement with the experimental values. For the S_1 state of both PSBT and PSB11, the TD-SVWN/6-311++G(d) predicted the closet S_1 T_v values as 598.4 and 602.9 nm to the 620 and 610 nm experimental values, respectively. The CASPT2//CASSCF(12,12)/6-31G(d) predicted T_v value of PSB11 S1 state is 545 nm.[18] However, the closest calculated 393.7 nm (396.8 nm) T_v values of PSBT (PSB11) S_2 state to the 385 nm (390 nm) experimental value is predicted by TD-B3LYP/6-31G(d). The TD-B3LYP method with 6-31G(d), 6-31+G(d), and 6-311++G(d) basis sets calculated f values of the PSBT and PSB11 S_1 states are about twice the corresponding S_2 ones, as shown in Table 1. But the other two TD-DFT methods predicted similar S_1 and S_2 f values. According to the "dark" S_2 state in experiment,[2] the TD-B3LYP predicted f values are more reliable.

For Linear Polyene oligomers, the TD-DFT/TDA performs considerably better for the excitation energies than TD-DFT itself.[43] We also calculated the T_v and f values of the PSBT and PSB11 S_1 and S_2 states using TD-B3LYP/TDA with 6-31G(d) and 6-311G(d) basis sets, respectively. Actually, the 6-31+

TABLE 1: TD-B3LYP and TDA Calculated Transition Energies (in nm) of the First Two Excited States of PSBT and PSB11, Compared with the Corresponding Experimental Values (Values in Parentheses are the Corresponding Calculated Oscillator Strengths)

	PSBT		PSB11	
method	S_1	S_2	S_1	S_2
exptl (from ref 2)	620	385	610	390
TD-B3LYP/6-31G(d)	536.1	393.7	539.5	396. 8
	(1.561)	(0.669)	(1.288)	(0.577)
TD-B3LYP/6-31+G(d)	543.1	397.3	546.6	400.0
	(1.580)	(0.647)	(1.295)	(0.564)
TD-B3LYP/6311++G(d)	543.9	398.1	548.1	401.3
	(1.579)	(0.646)	(1.291)	(0.561)
TD-BPW91/6-31G(d)	590.5	451.9	590.5	451.9
	(0.835)	(0.891)	(0.835)	(0.891)
TD-BPW91/6-31+G(d)	591.8	451.7	596.2	455.4
	(1.054)	(1.029)	(0.856)	(0.869)
TD-BPW91/6-311++G(d)	591.8	451.6	597.08	456.0
	(1.059)	(1.029)	(0.863)	(0.873)
TD-SVWN/6-31G(d)	592.3	451.1	596.1	454.7
	(1.003)	(1.058)	(0.8186)	(0.8895)
TD-SVWN/6-31+G(d)	598.3	455.4	602.1	458.65
	(1.040)	(1.026)	(0.845)	(0.866)
TD-SVWN/6-311++G(d)	598.4	455.7	602.9	459.2
	(1.043)	(1.024)	(0.851)	(0.878)
TD-B3LYP/TDA/6-31G(d)	472.0	365.1	478.3	368.3
	(2.043)	(1.977)	(1.706)	(1.654)
TD-B3LYP/TDA/TDA/6-311G(d)	477.0	368.2	482.1	371.0
	(2.067)	(1.909)	(1.718)	(1.597)

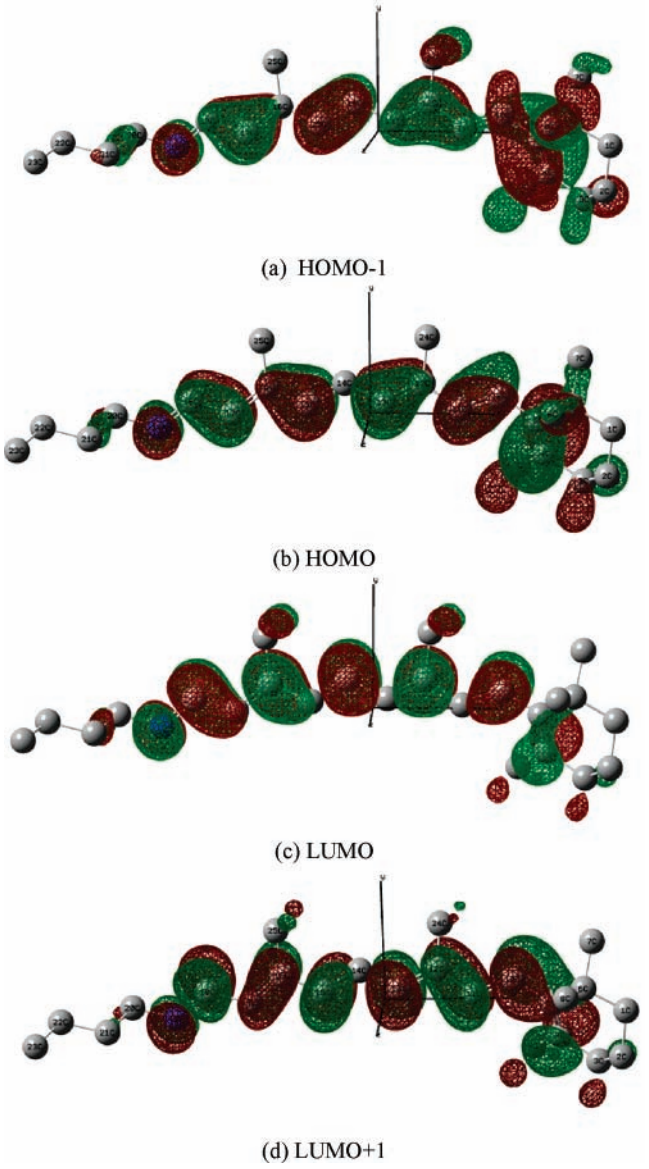

Figure 2. HOMO-1, HOMO, LUMO, and LUMO+1 plots of PSBT.

G(d) and 6-311++G(d) basis sets were also employed by the TD-B3LYP/TDA method but met problems of severe convergence and linear dependence of basis function. Anyway, all the above TD-DFT (including TD-B3LYP/TDA) calculations have proved that the basis set size has little influence on the excitation energies. Unfortunately, the TD-DFT/TDA method does not work well for our case. The TD-B3LYP/TDA/6-31G(d) predicated the T_v values of the PSBT (PSB11) S_1 and S_2 states to be 472.0 and 365.1 nm (478.3 and 368.3 nm), respectively, as shown in Table 1. As stated in ref 42, for the better TD-DFT/TDA result, "this must be viewed with caution because TD-DFT/TDA is itself an approximation to full TD-DFT".

To investigate whether the PSBT and PSB11 S_1 and S_2 states involve charge-transfer contributions, molecular orbital population analyses were made at the TD-B3LYP/6-31G(d) level. On the basis of the TD-B3LYP/6-31G(d) calculations, for the S_1 states of both PSBT and PSB11, two important transitions are highest-occupied molecular orbital (HOMO)-1→lowest-unoccupied molecular orbital (LUMO) and HOMO→LUMO+1, the former one is dominant as a percentage of about 77%. For the PSBT and PSB11 S_2 states, the two important transitions are HOMO-1→LUMO and HOMO→LUMO+1, and the former one is dominant by about 72%. The HOM-1, HOMO, LUMO, and LUMO+1 plots of PSBT and PSB11 were depicted Figures 2 and 3. According to the transition characters and the related molecular orbital plots, both the S_1 and S_2 states of PSBT and PSB11 are not typical charge-transfer states. This could be the reason that the TD-DFT/B3LYP/TDA method does not have advantage than the full TD-DFT ones in predicting the PSBT and PSB11 S_1 and S_2 excitation energies.

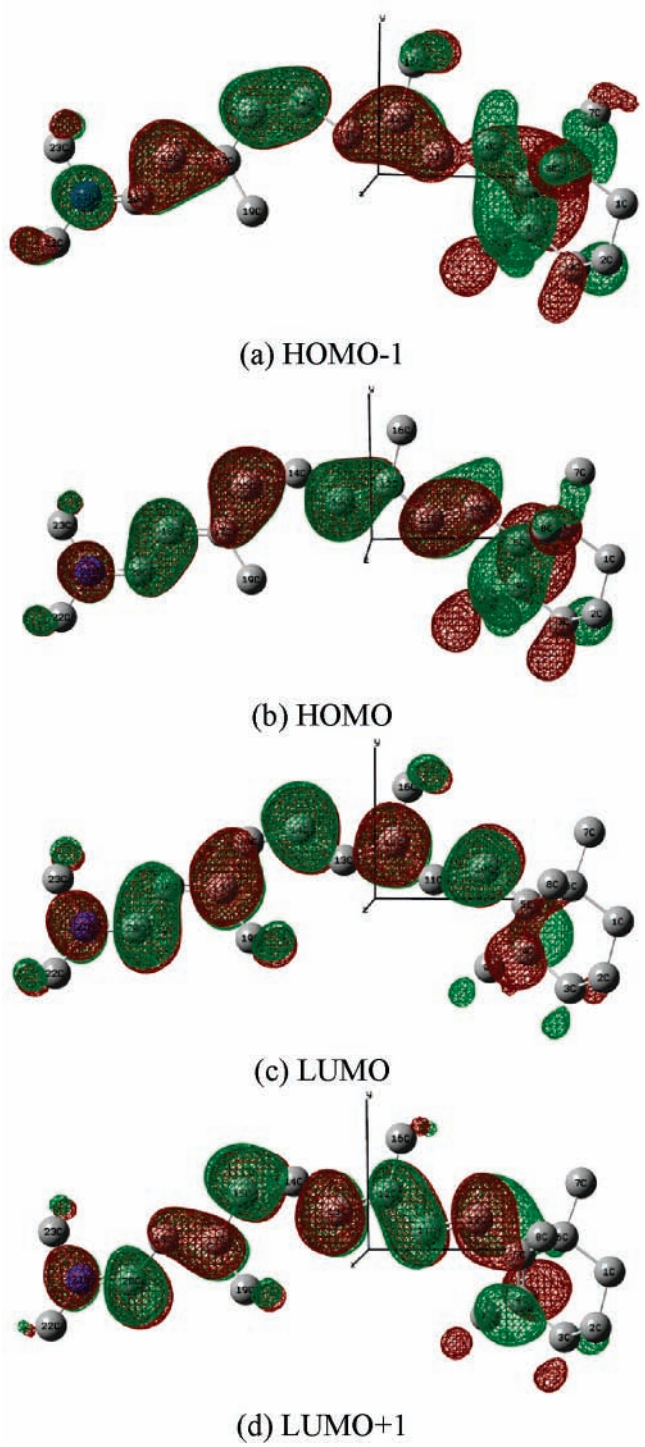

Figure 3. HOMO-1, HOMO, LUMO, and LUMO+1 plots of PSB11.

3.3. S_1 and S_2 Transition Dipole Moments. The following discussion is based on the TD-B3LYP/6-31G(d) calculated results. Since these discussions are actually qualitative, the basis set size hardly influences the calculated results as discussed above. The 3D cube representation of transition density can show the orientation of the transition dipole moment.[36−39] From

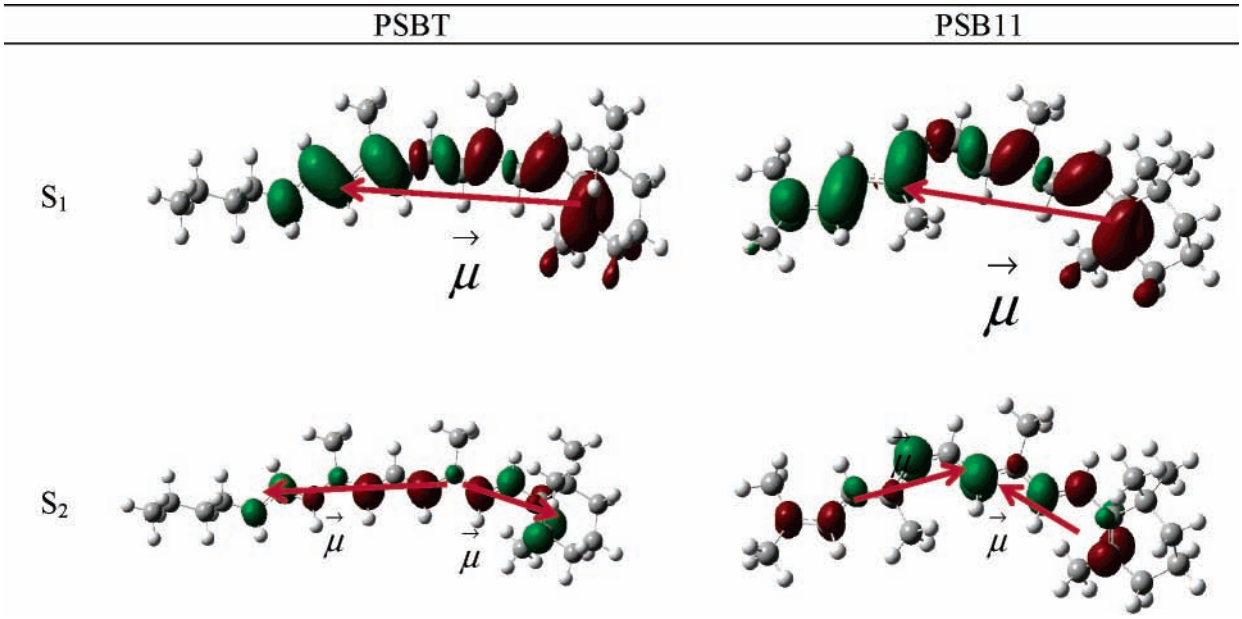

Figure 4. Transition densities of the PSBT and PSB11 S_1 and S_2 states. The green and red colors stand for hole and electron, respectively. The isovalue is 4×10^{-4} au. The orientation of the transition density is from the electron to the hole.

TABLE 2: TD-B3LYP/6-31G(d) Calculated Transition Electricity Dipole Moments (in au) of PSBT and PSB11 (Their Orientations are Depicted in Figure 1)

	PSBT			PSB11		
	X	Y	Z	x	y	z
S_1	−5.2240	0.4509	−0.0829	−4.6880	0.2511	0.2128
S_2	2.8931	0.5604	0.0204	2.7675	0.7455	−0.1745

TABLE 3: Fitted Changes in Transition Dipole Moments ($\Delta\mu$) and Polarizabilities ($\Delta\alpha$, au) on the Excitation for PSBT and PSB11

	PSBT		PSB11	
	Dm	Da	Dm	Da
S_1	1.60	0.00	1.84	−0.29
S_2	1.25	2.57	2.77	−2.85

the transition densities (see Figure 4), the transition dipole moments of S_1 are toward to the N^+ from the β-ionone ring for PSB11 and PSBT. For S_2 of both PSB11 and PSBT, there are two subtransition dipole moments ($\vec{\mu}_a$ and $\vec{\mu}_b$) with the opposite orientations, respectively, so the total transition dipole moments ($\vec{\mu}_{total}$) are smaller than any one of two subtransition dipole moments ($|\vec{\mu}_{total}| = |\vec{\mu}_a + \vec{\mu}_b| < |\vec{\mu}_a|and|\vec{\mu}_b|$). According to the relationship between transition dipole moment and oscillator strength, $|\mu|^2 \propto f/E$, the S_2 oscillator strengths become smaller, where E is the transition energy.[38,43] It should be noted that the two subtransition dipole moments of PSBT are "tail to tail", while the two of PSB11 are "head to head", and the physical reasons will be discussed later with the theory of nonlinear optical response. The calculated transition dipole moments for them were listed in Table 2, and the orientation of transition dipole moments can be seen from the geometries of the optimized ground state in Figure 4.

The optical properties of PSB11 and PSBT can be modulated over a wide range of wavelengths, based on the response of the retinal chromophore to external stress and the interaction with the charged, polar, and polarizable amino acids of the protein environment, which is connected to its large change in dipole moment upon excitation, its large electronic polarizability, and its structural flexibility.[19] To study the changes in absorption energies with the external electric field, the electric field strength dependent excitation energies were calculated, and the changes in dipole moment and polarizability were fitted with eq 1 by considering the external electric field strengths of 1×10^{-4}, 2×10^{-4}, and 3×10^{-4} au, and the fitted results were listed in Table 3. The choice of the orientation is along the x axis of the molecules (see Figure 4),[17] which is the orientation of the transition dipole moments (see Figure 3). For the PSBT S_1 state, the excitation energy is a linear optical (LO) response. For the PSB11 S_1 state, the excitation energy is almost a LO response, since $\Delta\alpha$ (0.29 au) is very small. While for the second excited state S_2 of PSBT, they are a nonlinear optical (NLO) response, because of large $\Delta\alpha$. The change in dipole moment of S_1 is larger than that of S_2 for PSBT but smaller for PSB11. It has been mentioned that for the S_2 excited-state of PSBT and PSB11, the two subtransition dipole moments of PSBT are "tail to tail", while the two subtransition dipole moment of PSB11 are "head to head", which can be interpreted by the different orientations of the change in the polarizability: the change in the polarizability during the $S_0 \rightarrow S_2$ transition is positive for PSBT, while negative for the PSB11.

4. Conclusions

The ground-state geometries of PSBT and PSB11 were optimized by B3LYP method with different size basis sets. Their S_1 and S_2 states' T_v and f values were calculated by TD-B3LYP, TD-BPW91, TD-SVWN, and TD-B3LYP/TDA with different size basis sets, respectively, on the corresponding B3LYP/6-31G(d) optimized ground-state geometries. The calculated results indicated that the basis set size hardly influences the geometrical optimizations and T_v and f calculations. The S_1 and S_2 of both PSBT and PSB11 are not charge-transfer states. It elucidates that TD-DFT/TDA is not always good in predicting excitation energies of such systems. All the calculations supported recently experimental reports about the three-state (S_0, S_1, and S_2) model. On the basis of the analyses on the transition densities and dipole moments, the phenomenon that S_2 being a "dark" state in spectroscopic for both PSBT and PSB11 was explained by its two subdipole moments oriented oppositely.

Acknowledgment. This work was supported by the Funding from the National Natural Science Foundation of China (Grant Nos. 10374040, 20673012, 10505001, 20060390017).

Supporting Information Available: Optimized geometries of PSB11 and PSBT. This material is available free of charge via the Internet at http://pubs.acs.org.

References and Notes

(1) Wald, G. *Science* **1968**, *162*, 230.
(2) Nielsen, I. B.; Lammich, L.; Andersen, L. H. *Phys. Rew. Lett.* **2006**, *96*, 018304.
(3) Andersen, L. H.; Nielsen, I. B.; Kristensen, M. B.; El Ghazaly, M. O. A.; Haacke, S.; Nielsen, M. B.; Petersen, M. Å. *J. Am. Chem. Soc.* **2005**, *127*, 12347.
(4) Bachilo, S. M.; Gillbro, T. *J. Phys. Chem. A* **1999**, *103*, 2481.
(5) Birge, R. R.; Murray, L. P.; Zidovetzki, R.; Knapp, H. M. *J. Am. Chem. Soc.* **1987**, *109*, 2090.
(6) Birge, R. R.; Murray, L. P.; Pierce, B. M.; Akita, H.; Baloghnair, V.; Findsen, L. A.; Nakanishi, K. *Proc. Natl. Acad. Sci. U.S.A.* **1985**, *82*, 4117.
(7) Mathies, R. A.; Brito Cruz, C. H.; Pollard, W. T.; Shank, C. V. *Science* **1988**, *240*, 777.
(8) Kandori, H.; Katsuta, Y.; Ita, M.; Sasabe, H. *J. Am. Chem. Soc.* **1995**, *117*, 2669.
(9) Hasson, K. C.; Gai, F.; Anfinrud, P. A. *Proc. Natl. Acad. Sci. U.S.A.* **1996**, *93*, 15124.
(10) Gonzalez-Luque, R.; Garavelli, M.; Bernardi, F.; Merchan, M.; Robb, M. A.; Olivucci, M. *Proc. Natl. Acad. Sci. U.S.A.* **2000**, *97*, 9379.
(11) Cembran, A.; Bernardi, F.; Olivucci, M.; Garavelli, M. *Proc. Natl. Acad. Sci. U.S.A.* **2005**, *102*, 6255.
(12) Yamamoto, S.; Wasada, H.; Kakitani, T. *THEOCHEM* **1998**, *451*, 151.
(13) Haupts, U.; Tittor, J.; Oesterhelt, D. *Annu. Rev. Biophys. Biomol. Struct.* **1999**, *28*, 367.
(14) Birge, R. R.; Bennett, J. A.; Hubbard, L. M.; Fang, H. L.; Pierce, B. M.; Kliger, D. S.; Leroi, G. E. *J. Am. Chem. Soc.* **1982**, *104*, 2519.
(15) Birge, R. R. *J. Chem. Phys.* **1990**, *92*, 7178.
(16) Kukura, P.; McCamant, D. W.; Yoon, S.; Wandschneider, D. B.; Mathies, R. A. *Science* **2005**, *310*, 1006.
(17) Schreiber, M.; Buss, V.; Sugihara, M. *J. Chem. Phys.* **2003**, *119*, 12045.
(18) Cembran, A.; Gonzalez-Luque, R.; Altoe, P.; Merchan, M.; Bernardi, F.; Olivucci, M.; Garavelli, M. *J. Phys. Chem. A* **2005**, *109*, 6597.
(19) Wanko, M.; Hoffmann, M.; Strodel, P.; Koslowski, A.; Thiel, W.; Neese, F.; Frauenheim, T.; Elstner, M. *J. Phys. Chem. B* **2005**, *109*, 3606.
(20) Wanko, M.; Garavelli, M.; Bernardi, F.; Niehaus, T. A.; Fraueheim, T.; Elstner, M. *J. Chem. Phys.* **2004**, *120*, 1674.
(21) Kohn, W.; Sham. L. J. *Phys. Rev.* **1965**, *140*, A1133.
(22) Hohenberg, P.; Kohn. W. *Phys. Rev.* **1964**, *136*, B864.
(23) Becke, A. D. *Phys. Rev. A* **1988**, *38*, 3098.
(24) Lee, C.; Yang, W.; Parr, R. G. *Phys. Rev. B* **1988**, *37*, 785.
(25) Petersson, G. A.; Al-Laham, M. A. *J. Chem. Phys.* **1991**, *94*, 6081.
(26) Petersson, G. A.; Bennett, A.; Tensfeldt, T. G.; Al-Laham, M. A.; Shirley, W. A.; Mantzaris, J. *J. Chem. Phys.* **1988**, *89*, 2193.
(27) McLean, A. D.; Chandler, G. S. *J. Chem. Phys.* **1980**, *72*, 5639.
(28) Krishnan, R.; Binkley, J. S.; Seeger, R.; Pople, J. A. *J. Chem. Phys.* **1980**, *72*, 650.
(29) Gross, E. K. U.; Kohn, W. *Phys. Rev. Lett.* **1985**, *55*, 2850.
(30) Perdew, J. P.; Chevary, J. A.; Vosko, S. H.; Jackson, K. A.; Pederson, M. R.; Fiolhais, C. *Phys. Rev. B* **1992**, *46*, 6671.
(31) Vosko, S. H.; Wilk, L.; Nusair, M. *Can. J. Phys.* **1980**, *58*, 1200.
(32) Slater, J. C. *Phys. Rev.* **1951**, *81*, 385.
(33) Frisch, M. J.; Trucks, G. W.; Schlegel, H. B.; Scuseria, G. E.; Robb, M. A.; Cheeseman, J. R.; Montgomery, J. A., Jr.; Vreven, T.; Kudin, K. N.; Burant, J. C.; Millam, J. M.; Iyengar, S. S.; Tomasi, J.; Barone, V.; Mennucci, B.; Cossi, M.; Scalmani, G.; Rega, N.; Petersson, G. A.; Nakatsuji, H.; Hada, M.; Ehara, M.; Toyota, K.; Fukuda, R.; Hasegawa, J.; Ishida, M.; Nakajima, T.; Honda, Y.; Kitao, O.; Nakai, H.; Klene, M.; Li, X.; Knox, J. E.; Hratchian, H. P.; Cross, J. B.; Adamo, C.; Jaramillo, J.; Gomperts, R.; Stratmann, R. E.; Yazyev, O.; Austin, A. J.; Cammi, R.; Pomelli, C.; Ochterski, J. W.; Ayala, P. Y.; Morokuma, K.; Voth, G. A.; Salvador, P.; Dannenberg, J. J.; Zakrzewski, V. G.; Dapprich, S.; Daniels, A. D.; Strain, M. C.; Farkas, O.; Malick, D. K.; Rabuck, A. D.; Raghavachari, K.; Foresman, J. B.; Ortiz, J. V.; Cui, Q.; Baboul, A. G.; Clifford, S.; Cioslowski, J.; Stefanov, B. B.; Liu, G.; Liashenko, A.; Piskorz, P.; Komaromi, I.; Martin, R. L.; Fox, D. J.; Keith, T.; Al-Laham, M. A.; Peng, C. Y.; Nanayakkara, A.; Challacombe, M.; Gill, P. M. W.; Johnson, B.; Chen, W.; Wong, M. W.; Gonzalez, C.; Pople, J. A. *Gaussian 03*, revision B.05; Gaussian, Inc.: Pittsburgh, PA, 2003.
(34) Hirata, S.; Head-Gordon, M. *Chem. Phys. Lett.* **1999**, *314*, 291.
(35) Apra, E.; Windus, T. L.; Straatsma, T. P.; Bylaska, E. J.; de Jong, W.; Hirata, S.; Valiev, M.; Hackler, M. T.; Pollack, L.; Kowalski, K.; Harrison, R. J.; Dupuis, M.; Smith, D. M. A.; Nieplocha, J.; Tipparaju, V.; Krishnan, M.; Auer, A. A.; Brown, E.; Cisneros, G.; Fann, G. I.; Fruchtl, H.; Garza, J.; Hirao, K.; Kendall, R.; Nichols, J. A.; Tsemekhman, K.; Wolinski, K.; Anchell, J.; Bernholdt, D.; Borowski, P.; Clark, T.; Clerc, D.; Dachsel, H.; Deegan, M.; Dyall, K.; Elwood, D.; Glendening, E.; Gutowski, M.; Hess, A.; Jaffe, J.; Johnson, B.; Ju, J.; Kobayashi, R.; Kutteh, R.; Lin, Z.; Littlefield, R.; Long, X.; Meng, B.; Nakajima, T.; Niu, S.; Rosing, M.; Sandrone, G.; Stave, M.; Taylor, H.; Thomas, G.; van Lenthe, J.; Wong, A.; Zhang, Z. *NWChem, A Computational Chemistry Package for Parallel Computers*, version 4.7; Pacific Northwest National Laboratory, Richland, Washington, 2005.
(36) Krueger, B. P.; Scholes, G. D.; Fleming, G. R. *J. Phys. Chem. B* **1998**, *102*, 5378.
(37) Beenken, W. J. D.; Pullerits, T. *J. Phys. Chem. B* **2004**, *108*, 6164.
(38) Sun, M. T. *J. Chem. Phys.* **2006**, *124*, 054903.
(39) Sun, M. T.; Kjellberg, P.; Beenken, W. J. D.; Pullerits, T. *Chem. Phys.* **2006**, *324*, 474.
(40) Grozema, F. C.; Telesca, R.; Jonkman, H. T.; Siebbeles, L. D. A.; Snijders, J. G. *J. Chem. Phys.* **2001**, *115*, 10014.
(41) Kjellberg, P.; He, Z.; Pullerits, T. *J. Phys. Chem. B* **2003**, *107*, 13737.
(42) Hsu, C. P.; Hirata, S.; Head-Gordon, M. *J. Phys. Chem. A* **2001**, *105*, 451.
(43) Sun, M. T. *Chem. Phys.* **2006**, *320*, 155.